Bioresource Technology 101 (2010) 4395–4402

Contents lists available at ScienceDirect

Bioresource Technology

journal homepage: www.elsevier.com/locate/biortech

Expression, purification and use of the soluble domain of *Lactobacillus paracasei* β-fructosidase to optimise production of bioethanol from grass fructans

C.M. Martel [a], A.G.S. Warrilow [a], C.J. Jackson [a], J.G.L. Mullins [a], R.C. Togawa [c], J.E. Parker [a], M.S. Morris [b], I.S. Donnison [b], D.E. Kelly [a], S.L. Kelly [a,*]

[a] *Institute of Life Science and School of Medicine, Swansea University, Swansea SA2 8PP, Wales, UK*
[b] *Institute of Biological, Environmental & Rural Sciences, Aberystwyth University, Gogerddan, Aberystwyth SY23 3EB, Wales, UK*
[c] *Embrapa Recursos Genéticos e Biotecnologia, Laboratório de Bioinformática, Parque Estação Biológica – Final W5 norte, Caixa Postal 02372, Brasília, DF 70770-900, Brazil*

ARTICLE INFO

Article history:
Received 15 October 2009
Received in revised form 13 January 2010
Accepted 19 January 2010
Available online 12 February 2010

Keywords:
Bioethanol
Fructan
Fructanase
Lactobacillus paracasei
Perennial ryegrass

ABSTRACT

Microbial inulinases find application in food, pharmaceutical and biofuel industries. Here, a novel *Lactobacillus paracasei* β-fructosidase was overexpressed as truncated cytosolic protein ($_t$fosEp) in *Escherichia coli*. Purified $_t$fosEp was thermostable (10–50 °C) with a pH optimum of 5; it showed highest affinity for bacterial levan (β[2-6] linked fructose) followed by nystose, chicory inulin, 1-kestose (β[2-1] linkages) and sucrose (K_m values of 0.5, 15, 15.6, 49 and 398 mM, respectively). Hydrolysis of polyfructose moieties in agriculturally-sourced grass juice (GJ) with $_t$fosEp resulted in the release of >13 mg/ml more bioavailable fructose than was measured in untreated GJ. Bioethanol yields from fermentation experiments with Brewer's yeast and GJ + $_t$fosEp were >25% higher than those achieved using untreated GJ feedstock (36.5[±4.3] and 28.2[±2.7] mg ethanol/ml, respectively). This constitutes the first specific study of the potential to ferment ethanol from grass juice and the utility of a novel core domain of β-fructosidase from *L. paracasei*.

1. Introduction

The use of plant biomass for the production of carbon–neutral biofuels continues to attract investment from research and commercial sectors (Larsen et al., 2008; Schmer et al., 2008). Industrially viable strategies to optimise the release of energy from cellulosic and lignocellulosic fractions of plant material (Hendriks and Zeeman, 2009 for recent review) continue to constitute a focal point for biofuel research (e.g. bioethanol from lignocellulosic biomass; Larsen et al., 2008). However, consideration of the complete spectrum of plant biomass that could be used for the production of bioethanol highlights additional reservoirs of carbon-energy; plant fructans comprise one of these sources.

In addition to sucrose and starch, fructans contribute to the pool of storage carbohydrates in plants (Ritsema and Smeekens, 2003). The simplest plant fructan is inulin which consists of a linear chain of β(2-1)-linked fructose monomers that extends from the fructosyl residue of a sucrose (α-β-1-2 linked glucose and fructose) starter molecule common to all plant fructans anabolised *in vivo*. Levan-type fructans also comprise a linear chain of fructose monomers; however these are linked via β(2-6) bonds. Finally, mixed-type fructans (gramminans) contain both β(2-1) and β(2-6)-linked fructose chains which can branch from the fructosyl and/or glucosyl residues of the sucrose starter molecule. Several fructan-containing plant crops including white clover (*Trifolium repens*), dandelion leaves (*Taraxacum* spp.), perennial ryegrass (*Lolium perenne* L.) and Jerusalem artichoke (*Helianthus tuberosus*) have been identified (see Kyazze et al., 2008). However, to date, few reports have been published on the production of bioethanol from plant fructans; those that are available tend to concentrate on the utilisation of *H. tuberosus* biomass (Nakamura et al., 1996; Szambelan et al., 2004). For example, it has been shown that inulin-type fructans derived from Jerusalem artichoke can be converted to ethanol by acidic hydrolysis followed by fermentation with *Saccharomyces cerevisiae* or via direct fermentation using *Kluyveromyces marxianus* strains (Negro et al., 2006). Similar research with a wider range of fructan-containing plant substrates is now required.

Given the total area (some 14 million hectares) of agricultural grassland in the UK (DEFRA, 2006), it is not surprising that perennial ryegrass has recently been identified as a possible substrate for the production of biofuels (Martinez-Perez et al., 2007). Unlike more specialist crops (e.g. wheat, sugar-beet) currently used for bioethanol production in Europe (Balat, 2007), ryegrass requires relatively few energy inputs (Donnison et al., 2009). Moreover, because of its fast establishment and robustness, ryegrass can be cultivated in marginal areas – an important consideration given the concerns surrounding use of arable land for non-food crops. The

* Corresponding author. Tel.: +44 1792 292207; fax: +44 1792 503430.
E-mail address: s.l.kelly@swansea.ac.uk (S.L. Kelly).

0960-8524/$ - see front matter Crown Copyright © 2010 Published by Elsevier Ltd. All rights reserved.
doi:10.1016/j.biortech.2010.01.084

direct microbial fermentation of ryegrass biomass to hydrogen has recently been reported (Kyazze et al., 2008). However, the potential to produce bioethanol from ryegrass remains under investigation.

The polyfructose moieties present in agriculturally-sourced ryegrass (*L. perenne*) biomass (Udén, 2006; Conaghan et al., 2008) require enzymatic hydrolysis to support yeast growth and bioethanol production. For this purpose we looked to produce a novel β-fructosidase enzyme derived from *Lactobacillus paracasei*. Of all the epiphytic lactic acid bacteria commonly found on grass (including perennial ryegrass), the fructan fermenters are typically strains of the species *L. paracasei* ssp. *paracasei* (Muller and Lier, 1994). An extracellular (42 kDa) fructanhydrolase displaying hydrolytic activity on levan, inulin and sucrose has already been purified from *L. paracasei* (Muller and Seyfarth, 1997) and it had been postulated that this might be the only fructan-degrading enzyme in *L. paracasei* (Muller and Seyfarth, 1997). However, a recent study of fructooligosaccharide utilisation has highlighted the presence of a second fructanhydrolase in *L. paracasei* (Goh et al., 2007). This β-fructosidase protein, the subject of experimental work reported hereafter, is a cell-wall anchored protein with an estimated molecular weight of 139 kDa (Goh et al., 2007).

L. paracasei β-fructosidase (*fosE*) was expressed here as a truncated cytosolic protein ($_t$fosEp) in *Escherichia coli* (lacking *N*′ secretion signal sequence and peptidoglycan binding domains). Following biochemical determinations (thermostability, pH profile and substrate specificity), purified fractions of the $_t$fosEp were used (alongside two commercial inulinases) to pre-treat grass juice. Bioethanol fermentation experiments with enzymatically hydrolysed grass juice were then undertaken using an ethanol tolerant brewing strain of *S. cerevisiae* as proof of principle to see if the novel soluble domain had potential for application. It was hypothesised that addition of $_t$fosEp to grass juice feedstock would result in fructan hydrolysis, increased bioavailability of fermentable fructose monomers, yeast growth and ultimately the production of bioethanol.

2. Methods

2.1. Expression and characterisation of recombinant β-fructosidase

2.1.1. Bacterial strains, plasmid and reagents

Plasmid pET17b (Novagen) and *E. coli* strain BL21 (DE3) (Novagen) were used for the expression of recombinant truncated β-fructosidase protein ($_t$fosEp). Enzymes for DNA manipulation were purchased from Promega (Madison, WI, USA) unless stated otherwise, all other reagents were purchased from Sigma (Poole, Dorset, UK).

2.1.2. Construction of recombinant plasmids

DNA primers were supplied by Invitrogen (Paisley, UK): F1 = 5′-ACGTA**CATATG**GCTAGCGCTACAAGTGCTTCGTCTAC-3′; R1 = 5′-ACGTA**GGATCC**TCA*GTGGTGGTGGTGGTGGTG*TTTTTCAGTTAGTTGACCAG-3′. F1 and R1 were used to amplify a truncated (*$_t$fosE*) gene (UniProtKB/TrEMBL [Q27J21_LACPA]) from *L. paracasei* genomic DNA omitting the amino acid residues 1–40 and 749–1376 which encode a predicted gram positive *N*′ secretion signal peptide (SignalP v3.0) and peptidoglycan cell wall binding regions at the *C*′ terminus (Pfam consensus PF06458 and Prosite consensus PS50847). The tripeptide sequence, Met–Ala–Ser, was inserted prior to the fosEp truncation site to assist heterologous expression. Specifically alanine is a preferred second codon for gene expression in *E. coli* (Barnes et al., 1991). A poly-histidine tag (italicised in primer R1) was included for Ni^{2+}–NTA agarose protein purification. The PCR fragment was cloned into pET17b using *Nde*I and *Bam*HI restriction sites (emboldened in primer sequences).

2.1.3. Expression and purification of recombinant β-fructosidase

E. coli strain BL21(DE3) harbouring the *$_t$fosE*–pET17b construct was cultured in Terrific broth supplemented with 0.1 mg/ml sodium ampicillin and 20 g/l peptone. Cultures were grown (37 °C, 230 rpm) for 7 h and expression was induced with 1 mM isopropyl β-D-thiogalactopyranoside (IPTG) for 18 h at 30 °C. Cells were harvested by centrifugation and sonicated in 0.1 M Tris-HCl (pH 8.1) containing 25% glycerol. The cytosolic fraction was isolated by removal of cell debris (20,000×*g*) and microsomes (150,000×*g*). The overexpressed $_t$fosEp was purified by affinity chromatography using Ni^{2+}–NTA agarose (Invitrogen). The purity of isolated $_t$fosE protein fractions was assessed by standard SDS polyacrylamide gel electrophoresis and protein identity confirmed by trypsin digestion and nano-LC/MS/MS analysis of a 100 kDa protein band (Pinnacle Laboratory; Newcastle University, UK). Protein concentrations were determined using the BioRad protein assay kit (BioRad, Hemel Hempstead, UK).

2.1.4. Biochemical characterisation of *$_t$fosEp*

Exo-inulinase activity was measured using a discontinuous assay system. One millilitre containing the saccharide of interest (dissolved in 0.1 M sodium acetate, pH 5) and the purified $_t$fosEp (≡1.62 μg protein/ml) was incubated for 30 min at 37 °C. A 0.1 ml volume from each reaction was then added to 0.9 ml 2,3,5-triphenyl tetrazolium chloride (1 mg/ml dissolved in 1 M NaOH), incubated at 37 °C for 15 min and the absorbance at 520 nm recorded. Fructose concentrations were determined relative to standards (0–6 mM fructose, in 0.1 M sodium acetate). The colorimetric reaction (Avigad et al., 1961) was found to be 20-fold more sensitive for D-fructose than D-glucose.

For thermostability determinations, stock solutions of the purified $_t$fosEp were heated for 10 min at temperatures ranging from 22 to 90 °C, cooled on ice for 5 min and assayed for residual exo-inulinase activity as described above using 10% (w/v) chicory inulin as substrate. The pH profile of the $_t$fosEp was determined using the exo-inulinase assay and 10% (w/v) chicory inulin dissolved in 0.1 M buffer solutions of sodium acetate (pH 3–6), sodium phosphate (pH 6.5–7.5), Tris–HCl (pH 8–8.5) or sodium bicarbonate (pH 9–11).

Substrate specificity for the $_t$fosEp was determined using chicory inulin (0.125–20% w/v), sucrose (0.025–2 M), 1-kestose (0.005–0.4 M), nystose (0.0045–0.35 M), raffinose (0.02–0.48 M), bacterial levan from *Zymomonas mobilis* (0.088–3.5% w/v), stachyose (0.04–0.4 M) and melezitose (0.04–0.4 M); all saccharides were dissolved in 0.1 M sodium acetate (pH 5) and assayed using the exo-inulinase system. For the determination of enzyme kinetic data, nominal molecular weights of 6200 and 12,000 Da were assumed for chicory inulin and bacterial levan, respectively.

2.1.5. Data processing and protein kinetics

DNA and protein sequences were processed using Chromas version 1.45, ClustalX version 1.8 and BioEdit version 5.0.6. Enzyme kinetics data were determined using the Michaelis–Menten equation: $v = (V_{max} \times [S])/(K_m + [S])$ and the Michaelis–Menten single substrate inhibition equation: $v = (V_{max} \times [S])/(k_m + ([S]^2/k_i) + [S]$. Curve-fitting was performed using ProFit 5.01 (QuantumSoft, Zurich, Switzerland). Enzyme activity is expressed as nkat/μg protein (equivalent to a reaction velocity of 60 nmol/min/μg protein).

2.2. Fermentation studies

2.2.1. Grass juice feedstock

Grass juice feedstock (hereafter GJ) extracted from the high-sugar perennial ryegrass *L. perenne* was supplied by the Institute of Biological, Environmental Research & Rural Sciences (IBERS, UK). Briefly, stands of *L. perenne* were maintained in 20 × 1.25 m plots under optimised management regimes (Wilkins et al., 2003). Vegetative

ryegrass was harvested in mid-June using a Haldrop plot harvester and juiced using a Green-Star™ GS1000 twin screw juicer (Savant Distribution Ltd., UK). *L. perenne* biomass was processed at 4 °C within 2 h of harvest; all GJ extracts were stored and transported in a frozen state. Residual fibrous grass material was also frozen for use in alternative crop research trials. The typical sugar, fructan and protein composition of *L. perenne* (cv. Aberdart) has been documented elsewhere (Udén, 2006; Conaghan et al., 2008).

In our laboratory, aliquots of GJ were screened to remove large particulates, filter-sterilised (Ministart, Sartorius, 0.2 μm) and frozen (−80 °C) prior to use as a growth and fermentation substrate. When required, particle-free GJ was thawed and used to prepare six feedstock media: media 1 = untreated GJ; media 2 = GJ + $_t$fosEp; media 3 = GJ + heat-denatured $_t$fosEp (GJ + $^{hd}_t$fosEp); media 4 = GJ + commercial exo-inulinase (GJ + Exo-I); media 5 = GJ + commercial endo-inulinase (GJ + Endo-I); media 6 = GJ + commercial exo- and endo-inulinase mixture (GJ + Exo/Endo-I). When added, commercial exo- and endo-inulinases from *Aspergillus niger* (Megazyme International Ireland Ltd.) or the $_t$fosEp (our laboratory) were used at a final concentration of 15 μg protein/ml (N.B. media 6 = 7.5 μg/ml of each inulinase). Following the addition of active enzymes (or the $^{hd}_t$fosEp) to GJ feedstock, 10 ml volumes were filter-sterilised and incubated (18 h, 37 °C, 180 rpm) to catalyse hydrolytic activity. To standardise all treatments, media 1 (untreated GJ) was supplemented with filter-sterilised water in place of enzyme/s. The concentrations of glucose in all media at t_0h (prior to the start of growth and fermentation experiments) were quantified using a glucose assay kit (GAGO-20, Sigma); fructose concentrations were estimated using the triphenyl tetrazolium chloride assay (Avigad et al., 1961).

2.2.2. Brewing strain and growth and fermentation experiments

Growth and fermentation studies were undertaken using Turbo yeast (Gert Strand AB, Sweden), a commercial brewing strain of *S. cerevisiae*. Turbo cultures were routinely cultured and maintained on YEPD medium containing (w/v): 2% glucose, 2% bacto-peptone and 1% yeast extract – including 2% agar when required (all media components supplied by Difco). Automated growth and fermentation experiments were performed in 100-well honeycomb microplates using a Bioscreen C (Oy Growth Curves Ab Ltd., Finland) to record changes in optical density (OD_{600}) over time. Uniform starting (t_0h) population densities (5×10^5 cells/ml) were achieved by adding yeast from overnight cultures (washed and diluted to 1×10^7 cells/ml) to the media of interest (50 μl cells + 950 μl media); the resulting 1 ml volumes were vortexed and aliquoted into 200 μl volume wells (four replicate wells per treatment). Semi-anaerobic fermentation conditions were achieved by sealing the microplates with lids and incubating them (without a shaking regime) at 20 °C in the Bioscreen. At t_{75}h estimations of the ethanol concentration (mg/ml) in each well were made using an ethanol assay kit (DIET-500) used in conjunction with a saccharide removal kit (DSRK-500, Bioassay Systems Ltd.). In addition to manual (Neubauer haemocytometer) cell counts at t_{75}h, optical density (OD) data were exported from the Bioscreen C in ASCII format and processed using Excel2003 (Microsoft Inc.). OD_{600} values were first corrected (by subtracting background OD_{600} for GJ); Excel2003 was then used to determine ΔOD values (maximum OD_{600} − minimum OD_{600}) between t_0h and t_{75}h. Student's *t*-tests were used to determine any levels of ethanol production and/or population growth that were significantly higher ($P < 0.05$) than those seen when Turbo yeast was grown on untreated GJ. All statistical analyses were performed using SPSS (Version 13.0).

2.3. Molecular modelling of L. paracasei β-fructosidase

Structural modelling was carried out using a homology modelling pipeline built with the Biskit structural bioinformatics platform (Grunberg et al., 2007) that peruses the entire Protein Databank of protein structures for putative structural homologues. The pipeline workflow incorporates the NCBI tools platform (Wheeler et al., 2008), including the BLAST program (Altschul et al., 1990) for similarity searching of sequence databases, T-COFFEE (Notredame et al., 2000) for alignment of the test sequence with the template, the MODELLER program (Eswar et al., 2003) for homology modelling, and the DSSP algorithm (Kabsch and Sander, 1983) for secondary structure validation. Homology models were generated with 10 iterations of the MODELLER program.

Alignment searching with the *L. paracasei* β-fructosidase sequence yielded 11 homologue structures (1ST8, 1UYP, 1W2T, 1Y4W, 1Y9G, 1Y9M, 2AC1, 2ADD, 2ADE, 2AEY, 2AEZ), filtered to the two with the best homology. A homology model was generated based on 31.7% sequence identity with the crystal structure of exo-inulinase from *Aspergillus awamori* (PDB: 1Y4W, chain A) (Nagem et al., 2004), and 29.4% identity with β-fructosidase from *Thermotoga maritima* (PDB: 1W2T, chain F) (Alberto et al., 2006). No homologue could be found for the sequence preceding residue 150. Structural models were visualized using the molecular graphics program Chimera (Pettersen et al., 2004).

3. Results

3.1. Expression and purification of the recombinant $_t$fosEp

Expression of $_t$*fosE* (Fig. 1) in *E. coli* yielded 22.5 nmoles/l of $_t$fosEp. SDS–PAGE indicated an apparent molecular weight of 100 kDa for recombinant $_t$fosEp (Fig. 2, lane 3). Although this is 20 kDa greater than the anticipated molecular weight of 81 kDa, altered gel mobility can be caused by a poly-histidine tail (Fig. 1). Trypsin digestion and nano-LC/MS/MS analysis of a 100 kDa $_t$fosE protein band identified 21 peptides that matched the deposited fosE protein sequence (Accession No. Q27J21). These accounted for 26% and 51% of the peptide composition of full-length and truncated fosE proteins; a Mascot score of 3609 (scores >1000 being largely unequivocal) confirmed the identity of $_t$fosEp.

3.2. Biochemical characterisation of the $_t$fosEp

Thermostability studies (Fig. 3A) indicated that the $_t$fosEp was stable up to 46 °C for 10 min. At temperatures higher than this pro-

```
MASATSASSTQISQTNTGSQPNNETTGETAQSSVNSTATA  40
SSSSVADLPSSSDSKSSIGSTISQPTVDKKETSKSDTADN  80
DLTKSVTTSDSDKALPTSKTTLPTSNEQVQSSVGQSQTDQ 120
PASSATIATNAVTSDVSQNDQYNEPYRNQYHYSSSQNWIN 160
DPNGLFYDSKTGLYNLYYQYNPEGNQWGNMSWGHAVSKDL 200
INWTQEDVAIPMLQNQGWEDFTYTNTTGSLKDKGEVRYVG 240
VPTTNWGDADGKKAIFSGSIVVDTNNVSGLGKDAILAFYT 280
ADYQIATRKNDGAEDGWGTWIGLTEIQEQHLAYSLDGGKT 320
FIQYSKDGNAANPQAIIPTSMNQGGDAANFRDPSVVYDAV 360
NKQYYLTVVSGQQALIYKSSNLLDWTYASKIERENDVGNG 400
VWECPSLVPMKVAGTNETKWVFCISVQQGAHATGSGMQYY 440
VGNMTADGTWVPESSKTLQNPMTMDSGEDFYAGIPFSNMP 480
DGRTVMLAWQSNWSYVDEAKTSPWSGNMTLPRELSLKKNA 520
DTTDGYLLTNTVVKEIANNEEANVINKAESNFTVSRSDEQ 560
VQYEGKQYKISATFSWDEADKPKSVGFKLRVSDDQKYDMI 600
VGYDLTTGLLYVQRLNTGEPNMGAPRDKMNATVNADGSIT 640
ITVYVDETSIEAFANDGEKSITQNFFMRPENIGDQATTGV 680
YVYSNDGTTKISDLTINPITSIWNSTGQLTEKHHHHHH*  718
```

Fig. 1. Amino acid sequence for the truncated *Lactobacillus paracasei* protein ($_t$fosEp). Peptide matches identified by nano-LC/MS/MS analysis of the purified $_t$fosEp are emboldened; double underlining highlights poly-histidine tag of the recombinant $_t$fosEp.

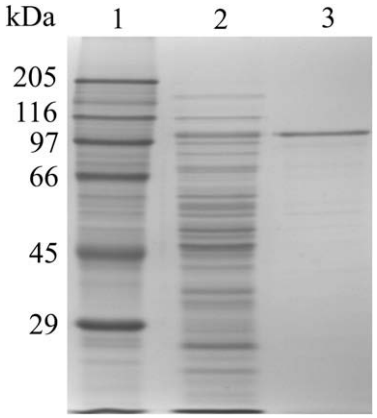

Fig. 2. SDS polyacrylamide gel electrophoresis of the purified $_t$fosEp. Lane 1 = molecular weight markers; lane 2 = all cytosolic proteins expressed in *E. coli*; lane 3 = the Ni^{2+}–NTA agarose purified $_t$fosEp.

tein activity was lost, with complete denaturation occurring >55 °C. The $T_{0.5}$ value for the $_t$fosEp was 49 °C under stated conditions. The pH profile of the $_t$fosEp (Fig. 3B) indicated an optimal pH of 5-5.5; protein activity declined sharply at pH values <5.0. The decrease in exo-inulinase activity at pH values >5.0 was more gradual; complete inactivation of the $_t$fosEp was not observed until pH 8 was exceeded.

Enzymatic hydrolysis of chicory inulin (glc:fru_n, β[2-1] linked fructose), levan (glc:fru_n, β[2-6] linkages), nystose (glc:fru_3, β[2-1] linkages), 1-kestose (glc:fru_2, β[2-1] linkages) and sucrose (glc:fru, α-β-1-2 bond) by the $_t$fosEp was observed (Table 1 and Fig. 3). Conversely the $_t$fosEp displayed negligible activity on raffinose and did not cleave fructose monomers from stachyose or melezitose (Table 1). Truncated fosEp had the greatest affinity for bacterial levan with a K_m value 30-fold less than that for inulin or nystose, 100-fold less than the K_m for 1-kestose and 800-fold less than the K_m for sucrose. The nystose results indicate a preference for a fructan chain length of two or more fructose residues. Levan concentrations above 3 mM were not used because of the viscosity of the solutions produced. Substrate inhibition was observed with both 1-kestose and inulin at concentrations above 100 and 12 mM, respectively, with calculated inhibition constants (K_i) of 210 and 13 mM for 1-kestose and inulin. In the case of inulin, part of the substrate inhibition observed may have been due to the increasing viscosity of the inulin solutions above 12 mM. V_{max} values obtained with inulin and 1-kestose were 3.45 and 1.55 nkat/μg $_t$fosEp whereas significantly lower V_{max} values of 0.66, 0.86 and 1.26 nkat/μg $_t$fosEp were obtained for nystose, levan and sucrose, respectively (Table 1). The low V_{max} value of just 0.07 nkat/μg $_t$fosEp obtained with raffinose indicated raffinose to be a particularly poor substrate. The maximum fructose turnover numbers observed using chicory inulin, nystose, levan, sucrose and 1-kestose were 106, 95, 89, 84 and 64 per second, respectively (Table 1). These results indicate that the $_t$fosEp has wide ranging substrate specificity and possesses exo-inulinase, exo-levanase and invertase activity.

3.3. Molecular modelling of $_t$fosEp

Structural molecular modelling (Fig. 5) indicated that the $_t$fosEp is composed almost entirely of beta strands and turns, and is predicted to possess only four very short helical regions. The beta

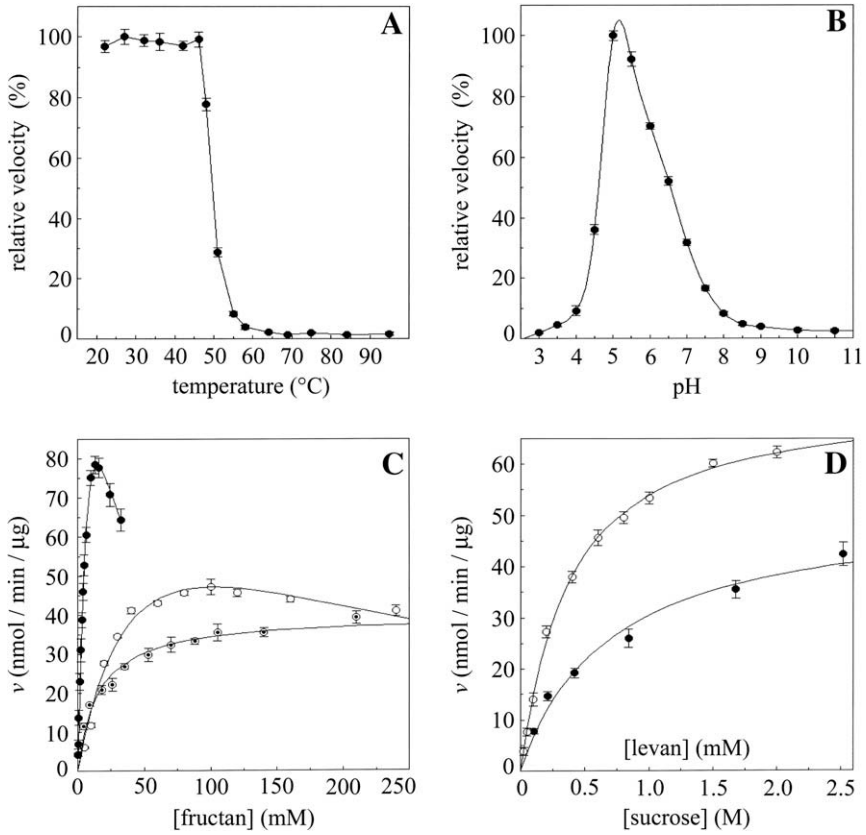

Fig. 3. Biochemical characterisation of the $_t$fosEp. Chicory inulin (10% w/v) was used to determine thermostability (A) and pH profiles (B). Substrate saturation curves for inulin (filled circles), 1-kestose (hollow circles) and nystose (bullets) were determined (C) along with levan (filled circles) and sucrose (hollow circles) (D). A velocity of 60 nmol/min/μg protein is equivalent to 1 nkat/μg protein; derived kinetic parameters are listed in Table 1.

Table 1
Substrate specificity of the $_t$fosEp. Mean values from at least three separate determinations are shown with standard deviations in brackets.

Substrate	Monosaccharide (glc:fru:gal)	Linkage (fru:fru)	MW (Da)	K_m (mM)	V_{max} (nkat/μg $_t$fosEp)	Turnover (fru/s)
Inulin	glc:fru$_n$	β(2-1)	6200	15.6[±3.1]	3.45[±0.52]	106[±15]
Levan	glc:fru$_n$	β(2-6)	12,000	0.5[±0.1]	0.86[±0.07]	89[±8]
Sucrose	glc:fru	None	342	398[±20]	1.26[±0.02]	84[±2]
1-Ketose	glc:fru$_2$	β(2-1)	504	49[±9.7]	1.55[±0.18]	64[±11]
Raffinose	glc:fru:gal	None	504	392[±130]	0.07[±0.02]	16[±2]
Nystose	glc:fru$_3$	β(2-1)	667	15[±2.1]	0.66[±0.02]	95[±3]
Stachyose	glc:fru:gal$_2$	None	667	–	0	0
Melezitose	glc$_2$:fru	None	504	–	0	0

structure forms two distinct domains. The first domain, corresponding to residues 151–580, possesses a characteristic central cavity and is separated from the smaller domain (residues 581–700) by a notable cleft that appears to be a conserved feature of all currently characterised fructanase structures (Nagem et al., 2004). By analysis of conservation of residues in other inulinases, levanases and invertases, the cleft region and the central cavity of the major domain are clearly implicated in the catalytic activity of the enzyme. Comparison of the sequences of enzymes with only β(2-6) activity and those with combined β(2-1) and β(2-6) activity suggests that the cleft region is particularly important for β(2-6) degradative activity; the central cavity appears to be more involved with β(2-1) degradative activity. A number of residues associated with determining substrate specificity are located in a region between the cavity and the cleft, in particular between residues 471–479.

3.4. Enzymatic pre-treatment of grass juice feedstock

Enzymatic pre-treatment of GJ feedstock (media 1–6, Table 2) prior to fermentation experiments with Turbo yeast (Fig. 4) resulted in differences in t_0h concentrations of bioavailable glucose and fructose. The activity of the $_t$fosEp on GJ (media 2) yielded the highest concentration of fructose (36.8[±4.1] mg/ml); this equates to >15 mg/ml (72.2%) more fructose than was measured in untreated GJ. Conversely, the combined action of commercial exo- and endo-inulinases on GJ (media 6, GJ + Exo/Endo-I), resulted in the highest initial concentration of glucose (8.8[±0.5] mg/ml);

Table 2
Summary of automated growth and fermentation experiments: A = total glucose and total fructose concentrations in media at t_0h; B = ethanol concentration, ΔOD and population density measurements at t_{75}h (maximum values emboldened). All (mean %) increases were calculated relative to untreated GJ (media 1). No residual glucose or fructose was detectable in fermented media at t_{75}h.

		Media					
		1 GJ	2 GJ + $_t$fosEp	3 GJ + $^{hd}_t$fosEp	4 GJ + Exo-I	5 GJ + Endo-I	6 GJ + Exo/Endo-I
A	*Glucose (mg/ml)*						
	Total[±SD]	7.9[0.4]	8.3[0.5]	8.0[0.4]	8.0[0.5]	8.5[0.5]	8.8[0.5]
	Increase (%)	–	(+5%)	(+1.3%)	(+1.3%)	(+7.6%)	(+11.4%)
	Fructose (mg/ml)						
	Total[±SD]	21.5[2.7]	36.8[4.1]	20.6[1.6]	30.5[1.6]	21.5[2.7]	27.8[1.6]
	Increase (%)	–	(+72.2%)	–	(+41.9%)	–	(+29.3%)
	Total fructose:total glucose	2.7:1	4.4:1	2.6:1	3.8:1	2.5:1	3.2:1
B	Total ethanol (mg/ml)	28.2[2.7]	36.5[4.3]	29.3[2.6]	32.1[3.5]	25.1[3.0]	31.6[4.0]
	Increase (%)	–	(+25.9%)	(+3.9%)	(+13.8%)	–	(+12.1%)
	ΔOD (600 nm)	1.43	1.5	1.44	1.52	1.39	1.52
	Density (cells/ml)	1.76×10^8	2.07×10^8	1.66×10^8	1.89×10^8	1.64×10^8	1.96×10^8

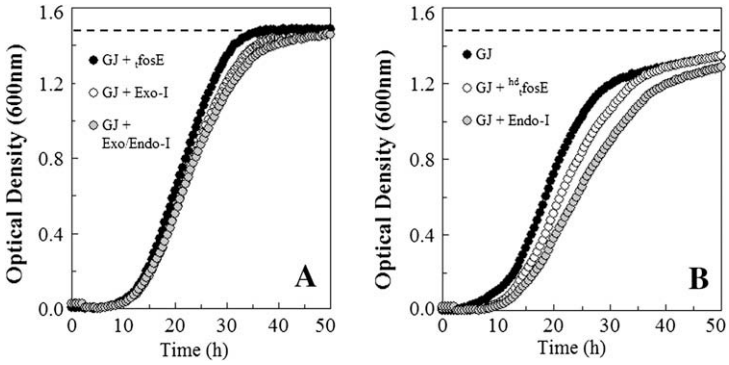

Fig. 4. Changes in optical density during automated growth and bioethanol fermentation experiments: A = growth of Turbo yeast on grass juice (GJ) pre-treated with the $_t$fosEp, commercial exo-inulinase or a mixture of commercial exo- and endo-inulinases; B = growth of Turbo yeast on untreated GJ, GJ pre-treated with heat-denatured $_t$fosEp or GJ treated with a commercial endo-inulinase. Broken line highlights maximum OD.

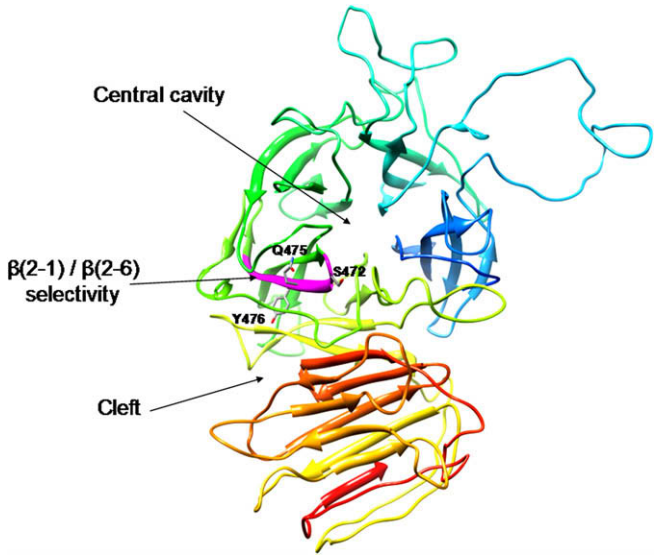

Fig. 5. Structural model of *Lactobacillus paracasei* (*fosE*) β-fructosidase showing the larger domain, (top, residues 150–580) with the characteristic central cavity and the smaller domain (bottom, residues 581–700), separated by the cleft that appears to be found in all fructanases (Nagem et al., 2004). The region implicated in substrate specificity (residues 471–479) is coloured in magenta with residues believed to be associated with breakage of β(2-6) linkages shown.

this corresponds to ≈1 mg/ml (11.4%) more glucose than was measured in untreated GJ. The highest (t_0h) total fructose:total glucose ratio was found in media 2 (GJ + $_t$fosEp) followed by GJ + Exo-I, GJ + Exo/Endo-I, GJ, GJ + $^{hd}_t$fosEp and finally GJ + Endo-I (ratios of 4.4, 3.8, 3.2, 2.7, 2.6 and 2.5:1, respectively). Bioavailable monosaccharides were utilised to completion for yeast growth and fermentation processes; no residual glucose or fructose were detectable in any of the GJ media at the end of fermentation studies (t_{75}h).

3.5. Growth and ethanol production on pre-treated and non-hydrolysed grass juice

As anticipated, GJ supplemented with the active $_t$fosEp (GJ + $_t$fosEp), exo-inulinase (GJ + Exo-I) and the exo/endo-inulinase enzyme mixture (GJ + Exo/Endo-I) supported greater yeast growth than untreated GJ, GJ + $^{hd}_t$fosEp and GJ + Endo-I (Fig. 4A and B). Addition of $^{hd}_t$fosEp to the feedstock (Table 2, media 3) did not result in higher OD values than those recorded on unsupplemented GJ; this indicates that $^{hd}_t$fosEp itself was not used as a growth substrate. Highest ethanol production was observed in growth experiments with GJ + $_t$fosEp followed by GJ + Exo-I, GJ + Exo/Endo-I, GJ + $^{hd}_t$fosEp, untreated GJ and finally GJ + Endo-I (mean ethanol concentrations of 35.5, 32.1, 31.6, 29.3, 28.2 and 25.1 mg/ml, respectively). Growth parameters (ΔOD values and cell counts) for Turbo populations grown on GJ + $_t$fosEp, GJ + Exo-I, and GJ + Exo/Endo-I were all significantly higher (Student's *t*-test, $P < 0.05$, $n = 3$) than those recorded on untreated GJ. However, only ethanol production on GJ + $_t$fosEp (not GJ + Exo-I or GJ + Exo/Endo-I) was found to be significantly higher than that seen on untreated GJ. A 25.9% increase in ethanol yield (relative to ethanol production on untreated GJ) was recorded with the GJ + $_t$fosEp feedstock; this equates to nearly double the next-highest increase (13.8%) seen in fermentation experiments with GJ + Exo-I (Table 2).

4. Discussion

Given the industrial applications and desirability of microbial inulinases (Chi et al., 2009), our results suggest that the $_t$fosEp is worthy of further investigation. Following successful expression as a cytosolic protein in *E. coli*, the purified $_t$fosEp was observed to hydrolyse chicory inulin, nystose and 1-kestose; all of these fructans comprise (inulin-series) chains of β(2-1) linked fructose. Enzymatic cleavage of bacterial (*Zymomonas mobilis*) levan (β[2-6] fructose linkages) and the α-β-1-2 bond (linking glucose [glc] and fructose [fru]) in sucrose was also seen. A part of the catalytic region between the cavity and the cleft (Fig. 5, residues 471–479) appears to be of particular interest in light of these activities as it contains seven residues conserved in β(2-1) linkage cleaving enzymes. Three of these residues, corresponding to Ser 472, Gln 475 and Tyr 476, are conspicuously different in *Aspergillus fumigatus* inulinase that is believed to only cleave β(2-6) linkages. This region may play an important role in determining substrate specificity of the enzyme, and emphasises the structural disposition of the *L. paracasei* enzyme toward wider substrate specificity.

That sucrose but not melezitose was hydrolysed (Table 1) suggests that the fructose unit in melezitose (glu_2:fru) might be shielded from $_t$fosEp activity by the presence of the second glucose unit linked (to fructose) at the C3 position. That hydrolysis of stachyose (a tetrasaccharide consisting of two α-galactose units, one α-glucose and one β-fructose) was not observed (Table 1) indicates that the $_t$fosEp possesses little or no α-galactosidase activity. Alpha-galactosidases cleave terminal α(1-6) linked galactose units from galacto-oligosaccharides of the raffinose family (Ulezlo and Zaprometova, 1982). Here, the minor hydrolytic activity observed on raffinose (a trisaccharide of glucose, fructose and galactose – formed by cleavage of one galactose from stachyose) suggests that the central fructose unit in raffinose might be accessible to the $_t$fosEp because it is not completely masked by the two terminal galactose moieties present in stachyose. Alternatively, it is possible that the $_t$fosEp acted upon sucrose impurities in the raffinose substrate.

Owing to its thermostability (10–50 °C) and pH optima (5.0–5.5), the $_t$fosEp displayed strong hydrolytic activity (at 37 °C for 18 h) on the fructan-rich grass juice feedstock (pH 5.5–5.7) used in growth and bioethanol fermentation experiments. Consideration of the (t_0h) glucose and fructose content of feedstock (media 1–6, Table 2) provides further information about both the saccharide composition of grass juice and the hydrolytic activity of $_t$fosEp. That proportionally more fructose than glucose was detected in media 3 (GJ + $_t$fosEp) suggests that the $_t$fosEp acted on fructan polymers (glc:fru_n and/or fru_n) and not simply free sucrose (glc:fru) in grass juice (theoretically, the hydrolysis of just sucrose would result in 1:1 increases of fru and glc). Moreover, (when compared to the commercial *A. niger* exo-inulinase used in this study) pre-treatment of grass juice with the $_t$fosEp resulted in the highest increase (relative to untreated GJ) in bioavailable fructose (increases of 72.2% and 41.9% for GJ + $_t$fosEp and GJ + Exo-I, respectively). Because the $_t$fosEp hydrolyses inulin- and levan-series fructans (β[2-1] and β[2-6] bonds respectively), its action on grass biomass which contains a mixture of these (Bonnett et al., 1994, 1997) is superior to (and in an industrial setting, might be preferable over) more specific commercial exo- and endo-inulinases. The addition of a commercial *A. niger* endo-inulinase (Endo-I) to grass juice (media 5) failed to increase the amount of free fructose available for fermentation at t_0h (Table 2). Endo-inulinases cleave non-terminal fructose-fructose bonds (i.e. in the middle of inulin chains); the by-product/s of endo-inulinase activity are thus short chain fructans and/or fructose dimers (Vogel, 1993). Importantly, these are neither detectable using the colorimetric assay employed in this study nor readily bioavailable for yeast growth and bioethanol production. This result indicates that the increased fructose content (at t_0h) in media 2, 4 and 6 owed primarily to exo-inulinase and (in the case of $_t$fosEp) invertase enzyme activity.

The experimental results from growth and fermentation studies reported here support our original hypothesis: that the addition of

the $_t$fosEp to GJ should result in (i) hydrolysis of polyfructose moieties (increasing fructose bioavailability), (ii) elevated levels of yeast population growth and iii) an increased yield of bioethanol. The ethanol yield (at t_{75}h) from fermentation of GJ + $_t$fosEp was significantly higher (Student's *t*-test, $P < 0.05$, $n = 3$) than that from untreated GJ (35.5 and 28.2 mg ethanol/ml respectively, Table 2). That ethanol production in control experiments (with GJ + $^{hd}{}_t$fosEp) was no higher than production seen on untreated GJ indicates that the $_t$fosEp itself was not utilised as a growth and fermentation substrate. It is noteworthy that (like GJ + $_t$fosEp) media 4 and 6 (GJ + Exo-I and GJ + Exo/Endo-I) supported significantly higher yeast growth (cell counts and ΔOD readings) but not ethanol production. This implies that the extra glucose and fructose made bioavailable by enzymatic hydrolysis of fructans in media 4 and 6 was sufficient to support yeast growth to stationary phase ($\approx 2.0 \times 10^8$ cells/ml), but not ethanol production during this phase. Conversely, the additional fructose released by the $_t$fosEp (>6.0 mg and 10 mg/ml more fructose than released by Exo-I and Exo/Endo-I) was adequate to support population growth to stationary phase and ethanol production thereafter.

The enzyme kinetics data and results from growth and fermentation experiments reported here, demonstrate the commercial potential of the $_t$fosEp as an enzyme capable of enhancing bioethanol yield from grass fructans. Given its broad substrate spectrum, pH optimum, thermostability and high fructose turnover rates the $_t$fosEp could also find application in alternative (e.g. food or pharmaceutical) industries (Chi et al., 2009). Obviously, the extent to which $_t$fosEp might increase bioethanol yield from grass juice is ultimately dependent on the composition of initial feedstock. Because the fructan content of ryegrass is under metabolic control, varying seasonally and with anthropogenic environmental stress (Cairns et al., 2008; Udén, 2006), experiments addressing the pre-treatment requirement/s of a variety of grass feedstocks are now needed. Work is also required to optimise fermentation conditions (e.g. the potential need for nutrient supplements) and to explore fermentation technologies (immobilised yeast strains, large-scale high gravity systems, etc.) that could enhance bioethanol yields from grass juice. Although this study focuses specifically on harnessing energy from the polyfructose component of ryegrass biomass, the emphasis of longer-term research is the utilisation of all (including fibrous) fractions of the grass crop for optimal bioethanol production. Attempts to achieve simultaneous saccharification and fermentation of grass juice using recombinant yeast that express microbial fructanases are currently underway.

Acknowledgements

Funding for this study was provided by the Welsh Energy Research Centre (WERC, UK) and the European Regional Development Fund of the European Union. Technical assistance was provided by Nicola Rolley (Swansea University, UK).

References

Alberto, F., Jordi, E., Henrissat, B., Czjzek, M., 2006. Crystal structure of inactivated *Thermotoga maritima* invertase in complex with the trisaccharide substrate raffinose. Biochemical Journal 395, 457–462.

Altschul, S.F., Gish, W., Miller, W., Myers, E.W., Lipman, D.J., 1990. Basic local alignment search tool. Journal of Molecular Biology 215, 403–410.

Avigad, G., Zelikson, R., Hestrin, S., 1961. Selective determination of sugars manifesting enediol isomerism by means of reaction with tetrazolium. Biochemical Journal 80, 57–61.

Balat, M., 2007. An overview of biofuels and policies in the European Union. Energy Sources Part B – Economics Planning and Policy 2, 167–181.

Barnes, H.J., Arlotto, M.P., Waterman, M.R., 1991. Expression and enzymatic-activity of recombinant cytochrome-p450 17-alpha-hydroxylase in *Escherichia coli*. Proceedings of the National Academy of Sciences of the United States of America 88, 5597–5601.

Bonnett, G.D., Sims, I.M., Stjohn, J.A., Simpson, R.J., 1994. Purification and characterization of fructans with beta-2,1-glycosidic and beta-2,6-glycosidic linkages suitable for enzyme studies. New Phytologist 127, 261–269.

Bonnett, G.D., Sims, I.M., Simpson, R.J., Cairns, A.J., 1997. Structural diversity of fructan in relation to the taxonomy of the Poaceae. New Phytologist 136, 11–17.

Cairns, A.J., Turner, L.B., Gallagher, J.A., 2008. Ryegrass leaf fructan synthesis is oxygen dependent and abolished by endomembrane inhibitors. New Phytologist 180, 832–840.

Chi, Z.M., Chi, Z., Zhang, T., Liu, G.L., Yue, L.X., 2009. Inulinase-expressing microorganisms and applications of inulinases. Applied Microbiology and Biotechnology 82, 211–220.

Conaghan, P., O'Kiely, P., Howard, H., O'Mara, F.P., Halling, M.A., 2008. Evaluation of *Lolium perenne* L. cv. AberDart and AberDove for silage production. Irish Journal of Agricultural and Food Research 47, 119–134.

DEFRA (e-Digest of Environmental Statistics), 2006. Environment Statistics and Indicators Division, Defra. Department for Environment, Food and Rural Affairs, UK. <www.defra.gov.uk>.

Donnison, I.S., Farrar, K., Allison, G.G., Hodgson, E., Adams, J., Hatch, R., Gallagher, J.A., Robson, P.R., Clifton-Brown, J.C., Morris, P., 2009. Functional genomics of forage and bioenergy quality traits in the grasses. Molecular Breeding of Forage and Turf 111, 123.

Eswar, N., John, B., Mirkovic, N., Fiser, A., Ilyin, V.A., Pieper, U., Stuart, A.C., Marti-Renom, M.A., Madhusudhan, M.S., Yerkovich, B., Sali, A., 2003. Tools for comparative protein structure modeling and analysis. Nucleic Acids Research 31, 3375–3380.

Goh, Y.J., Lee, J.H., Hutkins, R.W., 2007. Functional analysis of the fructooligosaccharide utilization operon in *Lactobacillus paracasei* 1195. Applied and Environmental Microbiology 73, 5716–5724.

Grunberg, R., Nilges, M., Leckner, J., 2007. Biskit – a software platform for structural bioinformatics. Bioinformatics 23, 769–770.

Hendriks, A., Zeeman, G., 2009. Pretreatments to enhance the digestibility of lignocellulosic biomass. Bioresource Technology 100, 10–18.

Kabsch, W., Sander, C., 1983. Dictionary of protein secondary structure – pattern-recognition of hydrogen-bonded and geometrical features. Biopolymers 22, 2577–2637.

Kyazze, G., Dinsdale, R., Hawkes, F.R., Guwy, A.J., Premier, G.C., Donnison, I.S., 2008. Direct fermentation of fodder maize, chicory fructans and perennial ryegrass to hydrogen using mixed microflora. Bioresource Technology 99, 8833–8839.

Larsen, J., Petersen, M.O., Thirup, L., Li, H.W., Iversen, F.K., 2008. The IBUS process – lignocellulosic bioethanol close to a commercial reality. Chemical Engineering & Technology 31, 765–772.

Martinez-Perez, N., Cherryman, S.J., Premier, G.C., Dinsdale, R.M., Hawkes, D.L., Hawkes, F.R., Kyazze, G., Guwy, A.J., 2007. The potential for hydrogen-enriched biogas production from crops: scenarios in the UK. Biomass and Bioenergy 31, 95–104.

Muller, M., Lier, D., 1994. Fermentation of fructans by epiphytic lactic-acid bacteria. Journal of Applied Bacteriology 76, 406–411.

Muller, M., Seyfarth, W., 1997. Purification and substrate specificity of an extracellular fructanhydrolase from *Lactobacillus paracasei* ssp *paracasei* P 4134. New Phytologist 136, 89–96.

Nagem, R.A.P., Rojas, A.L., Golubev, A.M., Korneeva, O.S., Eneyskaya, E.V., Kulminskaya, A.A., Neustroev, K.N., Polikarpov, I., 2004. Crystal structure of exo-inulinase from *Aspergillus awamori*: the enzyme fold and structural determinants of substrate recognition. Journal of Molecular Biology 344, 471–480.

Nakamura, T., Ogata, Y., Hamada, S., Ohta, K., 1996. Ethanol production from Jerusalem artichoke tubers by *Aspergillus niger* and *Saccharomyces cerevisiae*. Journal of Fermentation and Bioengineering 81, 564–566.

Negro, M.J., Ballesteros, I., Manzanares, P., Oliva, J.M., Sáez, F., Ballesteros, M., 2006. Inulin-containing biomass for ethanol production: carbohydrate extraction and ethanol fermentation. Applied Biochemistry and Biotechnology 129–132, 922–932.

Notredame, C., Higgins, D.G., Heringa, J., 2000. T-Coffee: a novel method for fast and accurate multiple sequence alignment. Journal of Molecular Biology 302, 205–217.

Pettersen, E.F., Goddard, T.D., Huang, C.C., Couch, G.S., Greenblatt, D.M., Meng, E.C., Ferrin, T.E., 2004. UCSF chimera – a visualization system for exploratory research and analysis. Journal of Computational Chemistry 25, 1605–1612.

Ritsema, T., Smeekens, S., 2003. Fructans: beneficial for plants and humans. Current Opinion in Plant Biology 6, 223–230.

Schmer, M.R., Vogel, K.P., Mitchell, R.B., Perrin, R.K., 2008. Net energy of cellulosic ethanol from switchgrass. Proceedings of the National Academy of Sciences of the United States of America 105, 464–469.

Szambelan, K., Nowak, J., Czarnecki, Z., 2004. Use of *Zymomonas mobilis* and *Saccharomyces cerevisiae* mixed with *Kluyveromyces fragilis* for improved ethanol production from Jerusalem artichoke tubers. Biotechnology Letters 26, 845–848.

Udén, P., 2006. In vitro studies on microbial efficiency from two cuts of ryegrass (*Lolium perenne*, cv. Aberdart) with different proportions of sugars and protein. Animal Feed Science and Technology 126, 145–156.

Ulezlo, I.V., Zaprometova, O.M., 1982. Microbial alpha-galactosidase (a review). Prikl Biokhim Mikrobiol 18, 3–15.

Vogel, M., 1993. A process for the production of inulin and its hydrolysis products from plant material. In: Fuchs, A. (Ed.), Inulin and Inulin-Containing Crops. Elsevier, Amsterdam, pp. 65–75.

Wheeler, D.L., Barrett, T., Benson, D.A., Bryant, S.H., Canese, K., Chetvernin, V., Church, D.M., DiCuccio, M., Edgar, R., Federhen, S., Feolo, M., Geer, L.Y., Helmberg, W., Kapustin, Y., Khovayko, O., Landsman, D., Lipman, D.J., Madden, T.L., Maglott, D.R., Miller, V., Ostell, J., Pruitt, K.D., Schuler, G.D., Shumway, M., Sequeira, E., Sherry, S.T., Sirotkin, K., Souvorov, A., Starchenko, G., Tatusov, R.L., Tatusova, T.A., Wagner, L., Yaschenko, E., 2008. Database resources of the national center for biotechnology information. Nucleic Acids Research 36, D13–D21.

Wilkins, P.W., Lovatt, M.L., Jones, M.L., 2003. Improving annual yield of sugars and crude protein by recurrent selection within diploid ryegrass breeding populations, followed by chromosome doubling and hybridisation. Czech Journal of Genetics and Plant Breeding 39, 95–99.